Front. Environ. Sci. Eng. 2018, 12(4): 5
https://doi.org/10.1007/s11783-018-1049-4

RESEARCH ARTICLE

Simultaneously recovering electricity and water from wastewater by osmotic microbial fuel cells: Performance and membrane fouling

Yuqin Lu[1], Xiao Bian[2], Hailong Wang[1], Xinhua Wang (✉)[1], Yueping Ren[1], Xiufen Li (✉)[1]

1 Jiangsu Key Laboratory of Anaerobic Biotechnology, School of Environmental and Civil Engineering, Jiangnan University, Wuxi 214122, China
2 School of Environment, Tsinghua University, Beijing 100084, China

HIGHLIGHTS

- OsMFC can simultaneously recover electricity and water from wastewater.
- Membrane fouling played an important role in flux decline of FO membrane in OsMFCs.
- Biofouling was the major fouling of the FO membrane in OsMFCs.
- The growth of biofouling layer on the FO membrane can be divided into three stages.
- Microorganisms were the dominant biofoulant in the biofouling layer.

GRAPHIC ABSTRACT

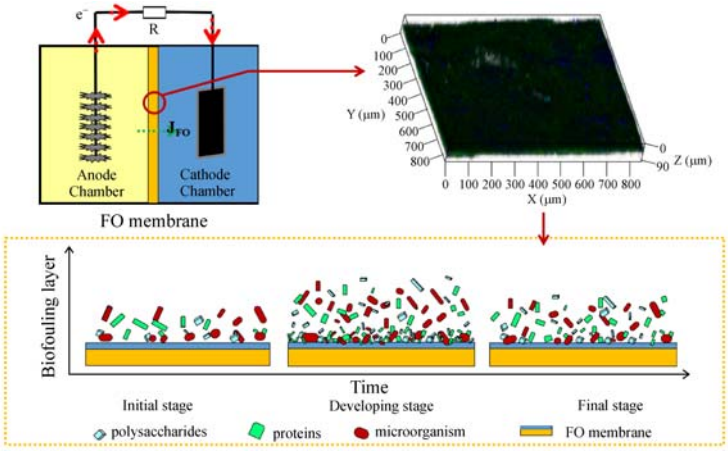

ARTICLE INFO

Article history:
Received 24 December 2017
Revised 22 March 2018
Accepted 24 May 2018
Available online 30 June 2018

Keywords:
Microbial fuel cell
Forward osmosis
Membrane fouling
Biofouling
Wastewater treatment

ABSTRACT

Since the concept of the osmotic microbial fuel cell (OsMFC) was introduced in 2011, it has attracted growing interests for its potential applications in wastewater treatment and energy recovery. However, forward osmosis (FO) membrane fouling resulting in a severe water flux decline remains a main obstacle. Until now, the fouling mechanisms of FO membrane especially the development of biofouling layer in the OsMFC are not yet clear. Here, the fouling behavior of FO membrane in OsMFCs was systematically investigated. The results indicated that a thick fouling layer including biofouling and inorganic fouling was existed on the FO membrane surface. Compared to the inorganic fouling, the biofouling played a more important role in the development of the fouling layer. Further analyses by the confocal laser scanning microscopy (CLSM) implied that the growth of biofouling layer on the FO membrane surface in the OsMFC could be divided into three stages. Initially, microorganisms associated with β-D-glucopyranose polysaccharides were deposited on the FO membrane surface. After that, the microorganisms grew into a biofilm caused a quick decrease of water flux. Subsequently, some of microorganisms were dead due to lack of nutrient source, in the meantime, polysaccharide and proteins in the biofouling layer were decomposed as nutrient source, thus leading to a slow development of the biofouling layer. Moreover, the microorganisms played a significant role in the formation and development of the biofouling layer, and further studies are needed to mitigate the deposition of microorganisms on FO membrane surfaces in OsMFCs.

© Higher Education Press and Springer-Verlag GmbH Germany, part of Springer Nature 2018

✉ Corresponding authors
E-mail: xhwang@jiangnan.edu.cn (Wang X H); xfli@jiangnan.edu.cn (Li X F)

Special Issue—Bio-based Technologies for Resource Recovery (Responsible Editors: Aijie Wang & David Stuckey)

1 Introduction

The concept of osmotic microbial fuel cells (OsMFCs) was proposed in 2011 (Zhang et al., 2011). In OsMFCs, the forward osmosis (FO) membrane was applied for replacing

the proton exchange membrane commonly used in traditional MFCs. Owing to the addition of FO membrane, OsMFC has higher quality of the effluent water, lower investment and larger bio-electricity generation compared with conventional MFCs for municipal wastewater treatment (Pant et al., 2010; Zhang et al., 2011; Ge and He, 2012; He, 2012; Ge et al., 2013; Li et al., 2014).

Previous studies have demonstrated that the quality of the effluent water and energy recovery in the OsMFC were better than that in the conventional MFC (Pant et al., 2010; Zhang et al., 2011; Ge and He, 2012; He, 2012; Ge et al., 2013; Werner et al., 2013; Li et al., 2014; Qin et al., 2015). According to these literature, compared with the traditional MFCs, the electricity generation is improved in the OsMFC owing to the accelerated ion transport resulting from the osmotic pressure difference, and the product water quality was absolutely enhanced due to the high rejection of FO membrane (Ge and He, 2012; Ge et al., 2013; Werner et al., 2013; Qin et al., 2015). Although the OsMFC had many advantages over the traditional MFC, it has a main drawback, i.e., a low water flux of FO membrane in the range of 1.22-4.10 LMH (Zhang et al., 2011; Ge and He, 2012; Ge et al., 2013; Werner et al., 2013). A low FO membrane flux led to many problems including frequently washing for recovering permeability, low efficiency of producing electricity, large operating cost, etc. According to previous studies on FO membrane technology (Cath et al., 2006; Mccutcheon and Elimelech, 2006; Pant et al., 2010; Tang et al., 2010; Ge et al., 2013; Werner et al., 2013; Qin et al., 2015; Wang et al., 2016a), the lower water flux was most likely due to membrane fouling, concentration polarization and operating conditions. At present, the research on OsMFC is mainly focused on the construction of the device and the optimization of its operating conditions. Considering the significant impacts of membrane fouling on the operating flux of FO membrane, it is necessary to investigate the fouling behaviors in the OsMFCs.

According to previous reports on the FO membrane applied for wastewater treatment (Mi and Elimelech, 2008; Ge et al., 2013; Wang et al., 2014a, 2014b, 2017c; Yuan et al., 2015; Zhu et al., 2018), its fouling tendency is moderate, and its permeability can be recovered just by the physical cleaning. However, recent studies have demonstrated that the FO membrane fouling is severer when it is applied in an anaerobic condition (Chen et al., 2014; Liu et al., 2017; Wang et al., 2017a, 2017b, 2018). Regardless of the fouling extent of FO membrane, the fouling was complicated, and the foulants includes microorganisms, organic and inorganic matters (Xie et al., 2015; Yuan et al., 2015; Wang et al., 2017b). If the FO membrane combined with biotechnology such as aerobic and anaerobic sludge for wastewater treatment, the biofoulants are the dominant foulants on the FO membrane surface (Wang et al., 2017a, 2017b). Although many studies have focused on the FO membrane fouling during wastewater treatment, the reports on the fouling behaviors of FO membrane in OsMFCs are limited. Until now, just the following four publications have reported the FO membrane fouling in OsMFCs. Ge et al. (2013), Werner et al. (2013) and Zhu et al. (2016) observed the similar fouling behavior of FO membrane in OsMFCs, i.e., a dense fouling layer was formed by bacteria, EPS and inorganic components on the membrane surface. Based on the above results, some researchers have used silver nanoparticles to modify the surface of FO membrane for mitigating the membrane fouling in OsMFCs (Yang et al., 2016). Although these publications are helpful for understanding the FO membrane fouling in OsMFCs, the systematical fouling mechanisms especially the development of fouling layer of FO membrane are not yet clear. Thus, the objectives of this study are to systematically study on membrane fouling combined organic, inorganic and biofouling in the context of OsMFC and preliminary understand the development of the biofouling layer. To the best knowledge of the authors, this is the first study focused on the development of the biofouling layer on the FO membrane surface in OsMFCs.

2 Materials and methods

2.1 Set-up and operating condition

A laboratory scale OsMFC (see Fig. 1) with an FO membrane installed between anode and cathode compartments was applied in this study. The FO membrane with an effective membrane area of 48 cm^2 was made of thin film composite polyamide (TFC) (Hydration Technologies Inc.), and its orientation of active layer facing the feed solution (AL-FS) was applied in this study. Each compartment had an effective volume of 144 mL. A pretreated carbon brush (JT-300A-1K, Jilin Shenzhou Carbon Fiber Company, China) was inserted into the anode compartment as the anode electrode, and the cathode electrode was a piece of carbon cloth coasted with Pt as the catalyst (0.3 mg/cm^2) prepared as previously (Zhang et al., 2010). The draw solution tank coupled with a magnetic stirrer for supplying oxygen from air to finish the reaction on cathode. The anode and cathode electrodes were connected through a 500 Ω resister. The cell voltage was recorded every 5 min by a data acquisition system (RBH8221, Ruibohua Co., China).

During the operation of OsMFC, the synthetic wastewater was continuously recycled from the buffer tank to the anode compartment with a flow rate of 87.5 mL/min (a corresponding cross-flow velocity of 0.03 cm/s). The draw solution of 0.5 M NaCl was recirculated at the same flow rate. The synthetic wastewater contained 230 mg/L glucose, 60 mg/L peptone, 40 mg/L CH_3COONa, 20 mg/L beef paste, 198 mg/L $NaHCO_3$, 12 mg/L KH_2PO_3, 170 mg/L NH_4HCO_3, 2.4 mg/L $MgCl_2 \cdot 6H_2O$, 1.2 mg/L $CaCl_2$ and 1 mg/L $FeCl_3 \cdot 6H_2O$, and its concentrations of

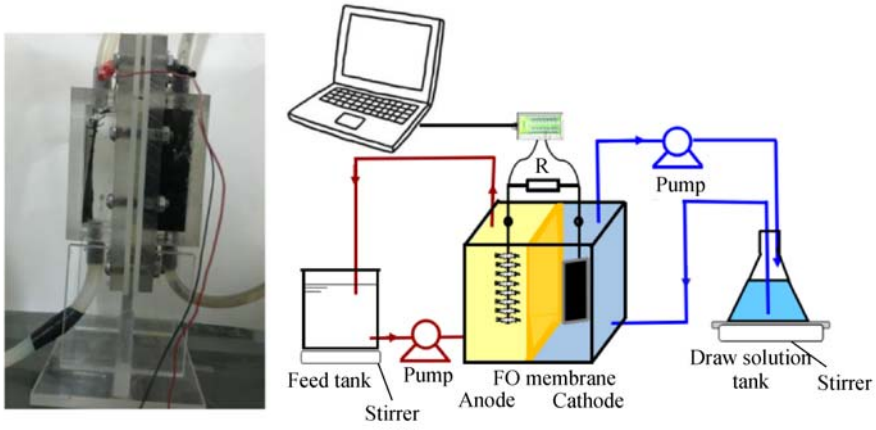

Fig. 1 Schematic diagram of the OsMFC

chemical oxygen demand (COD), total organic carbon (TOC), ammonia nitrogen (NH_4^+-N), total nitrogen (TN) and total phosphorus (TP) were 374.8±9.2, 116.2±6.64, 30.2±0.59, 32.4±1.92 and 2.90±0.18 mg/L, respectively. The seeded sludge was collected from a local domestic wastewater treatment plant (Taihu Xincheng Wastewater Treatment Plant, Wuxi, China). The initial mixed liquor suspended solids (MLSS) and mixed liquor volatile suspended solids (MLVSS) of the sludge in the OsMFC were 3.1 and 2.0 g/L, respectively. When the max output voltage and the operating time of one cycle were stable, the OsMFC finished the start-up. During the whole experiment, the temperature was controlled at 30°C±0.5°C.

2.2 Analytical methods

Water flux through the FO membrane was calculated based on the volume change of the draw solution, and the conductivity of anolyte and catholyte were recorded by a conductivity meter (OKD-650, Shenzhen OK Instrument Technology Co., Ltd., China). NH_4^+-N, TN and TP in the influent, anolyte and catholyte were determined according to the APHA standard methods (2012), and TOC was measured using a TOC Analyzer (Shimadzu TOC-Vcsh, Japan).

The polarization curve was performed by varying the circuit external resistance from 68 to 33,000 Ω, and the internal resistance (R_{int}) was calculated from the slope of the linear region of the polarization curve (Logan et al., 2006). The volumetric densities of power and current were calculated based on the liquid volume of the anode compartment.

The foulants on the FO membrane surface were collected by the method described by Wang et al. (2017b), and then the MLSS and MLVSS concentrations of the foulants were determined according to the APHA Standard Methods (2012). An energy diffusive X-ray (EDX) (Falcon, EDAX Inc., America) and a scanning electron microscopy (SEM) (S-4800, Hitachi, Japan) were applied for analyzing the element compositions and capturing the surface images of the virgin and fouled FO membranes, respectively. A confocal laser scanning microscopy (CLSM) (ZEISS LSM 710, ZEISS, Germany) was used for observing the distributions of biofoulants including microorganisms, proteins and polysaccharides on the fouled FO membrane samples. The obtained images were analyzed by the ZEN software, and the biovolume was calculated by a software of Auto PHLIP-ML (version 1.0). The specific methods of SEM, EDX and CLSM analyses could be found in previous literature (Wang et al., 2014a, 2016b; Yuan et al., 2015).

2.3 Mass balance

The TOC, NH_4^+-N, TN and TP concentrations in the FO permeate (C_{FO}, mg/L) and their rejection by the FO membrane (R, %) could be calculated according to the Eqs. (1) and (2), respectively.

$$C_{FO} = \frac{C_{Fin}^{Cat} V_{Fin}^{Cat}}{C_{Ini}^{Cat} V_{Ini}^{Cat}}, \quad (1)$$

$$R = \left(1 - \frac{C_{FO}}{C_{Ini}^{Ano}}\right) \times 100\%, \quad (2)$$

where C_{Ini}^{Cat} and C_{Fin}^{Cat} are the initial and final contaminant concentrations of the catholyte (mg/L, C_{Ini}^{Cat} = 0 mg/L), respectively, V_{Ini}^{Cat} and V_{Fin}^{Cat} are the initial and final catholyte volume (L, V_{Ini}^{Cat} = 0.5 L), respectively, and C_{Ini}^{Ano} is the initial contaminant concentration of the anolyte (mg/L).

The removal efficiencies of contaminants by the combination of microorganisms and FO membrane (η_T) and only by microorganisms (η_1) were calculated as given in the equations below.

$$\eta_T = \left(1 - \frac{C_{\mathrm{Fin}}^{\mathrm{Cat}} V_{\mathrm{Fin}}^{\mathrm{Cat}}}{C_{\mathrm{Ini}}^{Ano} V_{\mathrm{Ini}}^{\mathrm{Ano}}}\right) \times 100\%, \quad (3)$$

$$\eta_1 = \left(1 - \frac{C_{\mathrm{Fin}}^{\mathrm{Cat}} V_{\mathrm{Fin}}^{\mathrm{Cat}} + C_{\mathrm{Fin}}^{\mathrm{Ano}} V_{\mathrm{Fin}}^{\mathrm{Ano}}}{C_{\mathrm{Ini}}^{\mathrm{Ano}} V_{\mathrm{Ini}}^{\mathrm{Ano}}}\right) \times 100\%, \quad (4)$$

where $C_{\mathrm{Fin}}^{\mathrm{Ano}}$ is the final contaminant concentration of the anolyte (mg/L), and$V_{\mathrm{Ini}}^{\mathrm{Ano}}$ and $V_{\mathrm{Fin}}^{\mathrm{Ano}}$ are the initial and final anolyte volume (L, $V_{\mathrm{Ini}}^{\mathrm{Ano}}$ = 2.0 L), respectively.

3 Results and discussion

3.1 Performance of OsMFC

As shown in Fig. 2, voltage was produced in all cycles and the maximum voltage was 410 mV, which was slightly higher than previous studies on OsMFCs with external resistance of 10 Ω (Qin et al., 2015) and 100 Ω (Werner et al., 2013; Zhu et al., 2015). The batch operation exhibited a voltage profile affected by the organic substrate, i.e., the voltage increased upon the replacement of the anolyte and then decreased due to the depletion of the organic substrates. As shown in Fig. 2(b), the polarization test demonstrated the open circuit potential was 0.719 V, and the maximum power density was 2.62 W/m^3. Furthermore, the internal resistance of the OsMFC was approximately 353.37 Ω calculated from the slope of the polarization curve.

Figure 3 illustrates the variations of TOC, NH_4^+-N, TN and TP concentrations in the influent, anolyte, catholyte and FO permeate during the operation of OsMFC. From Fig. 3(a), the TOC concentration in the FO permeate was less than 4.0 mg/L with an average removal efficiency of more than 99.0% (Table S1, see it in Supplementary material) compared to the influent TOC concentration of approximately 116.2 mg/L. The high removal rate of TOC was attributed to the combining effects of the microorganisms in the anode chamber (96.6%) and the rejection of FO membrane (97.9%). High TOC removal efficiency in current study was consistent with previous MFCs treating low-strength wastewater (Ge et al., 2013; Werner et al., 2013). From Fig. 3(b) and Fig. 3(c), the concentrations of NH_4^+-N and TN in the FO permeate were 12.2±1.6 mg/L and 17.2±2.5 mg/L, respectively, with an average removal efficiency of 78.7% and 73.6% (Table S1), respectively. The TN removal of OsMFCs was mainly due to the rejection of FO membrane (Qin et al., 2017). With regard to the phosphorus removal, the average removal rate in anode compartment were 30.6% (Table S1) compared to the influent concentrations of 2.97±0.18 mg/L. Interestingly, it could be observed some crystal precipitation at the bottom of the anode compartment, which implied that the phosphorus might be combined with Ca^{2+} and/or Mg^{2+} to form precipitation. Owing to the high rejection of FO membrane, the average concentration of TP in the FO permeate was below 0.7 mg/L. Likely previous reports on OsMFCs, the OsMFC had better effluent quality compared to the traditional MFCs owing to the addition of FO membrane.

3.2 Performance of FO membrane

In each cycle, the salinity in the anode compartment increased due to the rejection of FO membrane for influent solutes and the reverse solute transport from the draw solution while it decreased in the cathode compartment owing to the dilution of FO permeate. However, the conductivity of anolyte in the end of each cycle was in a low range of 4.82−6.61 mS/cm (see Fig. 4) due to a slow salinity increase during a short running time. Furthermore, it could be seen from Fig. 4 that the final salinity in the anolyte and catholyte was relatively stable in all cycles of the OsMFC, suggesting that the operation of the OsMFC was similar in each cycle. Considering the lower salinity environment in the anode compartment, the salinity had no adverse effects on the water flux of FO membrane, the physical and biochemical properties of sludge and the

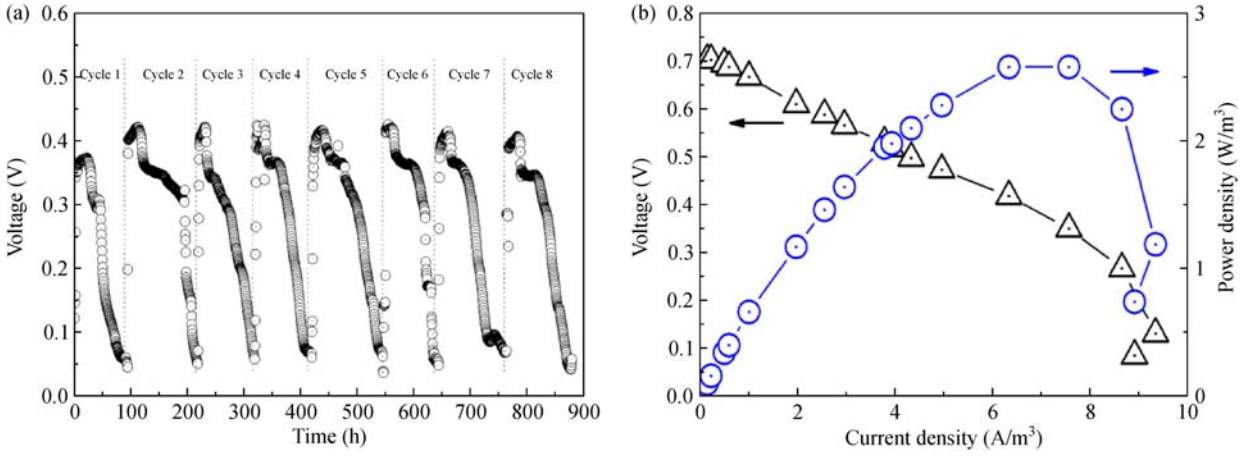

Fig. 2 Electricity generation (a), power density and polarization curves (b) of the OsMFC

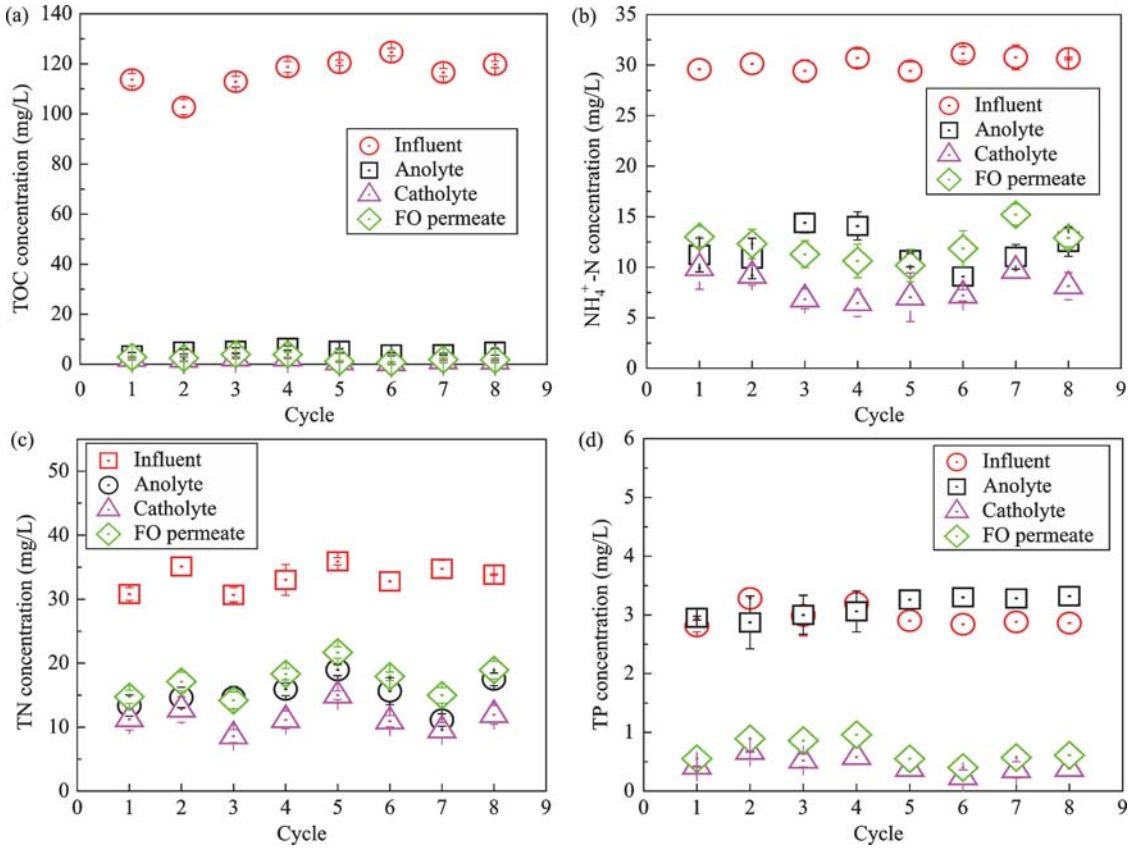

Fig. 3 Variations of TOC (a), NH_4^+-N (b), TN (c) and TP (d) concentrations in the influent, anolyte, catholyte and FO permeate in the end of each cycle

microbial activity (Mahan and Das, 2009; Lefebvre et al., 2012). Thus, it no need for controlling the salinity accumulation. In fact, the similar salinity variations could be observed in previous studies on OsMFCs applying an intermittent operation (Ge et al., 2013; Werner et al., 2013).

From Fig. 4, it could be observed that the water flux of FO membrane significantly reduced from 3.57 LMH to 1.53 LMH after 8 cycles. Considering the similar change of salinity in each cycle, the decline of FO membrane flux could be mainly attributed to the membrane fouling. Furthermore, it is interesting to note that the decline of FO membrane flux mainly happened in first three cycles, and then the flux was relatively stable. It might be implied that the foulants deposited on the FO membrane and formed a fouling layer in the first three cycles, and then the fouling layer developed slowly. Thus, it is necessary to further understand the fouling behavior of FO membrane in the OsMFC.

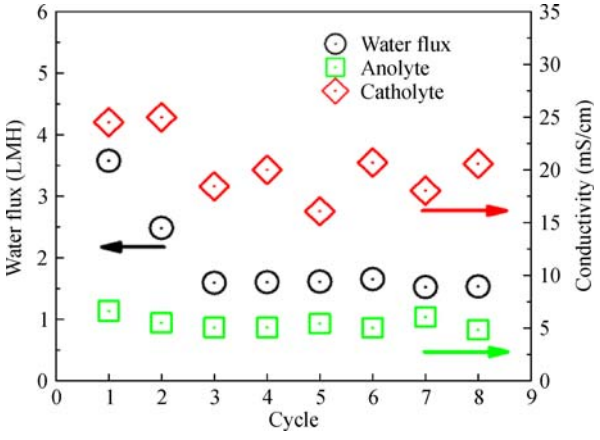

Fig. 4 Variations of water flux of the FO membrane and the conductivity of the anolyte and catholyte in the end of each cycle

3.3 Fouling observation of FO membrane

Compared to the virgin FO membrane, a fouling layer could be observed on the FO membrane surface after the OsMFC operating 8 cycles from the photo and SEM image (see Fig. 5). Previous studies have been reported that the existence of cake layer will severely decrease the mass transfer coefficient resulting in a serious flux decline (Zhang et al., 2012). It should be pointed out that the fouling layer could be easily removed just by washing with the tap water, indicating that the FO membrane fouling in the OsMFC was mainly due to the reversible fouling. Furthermore, the EDX results (Fig. 5 and Table S2)

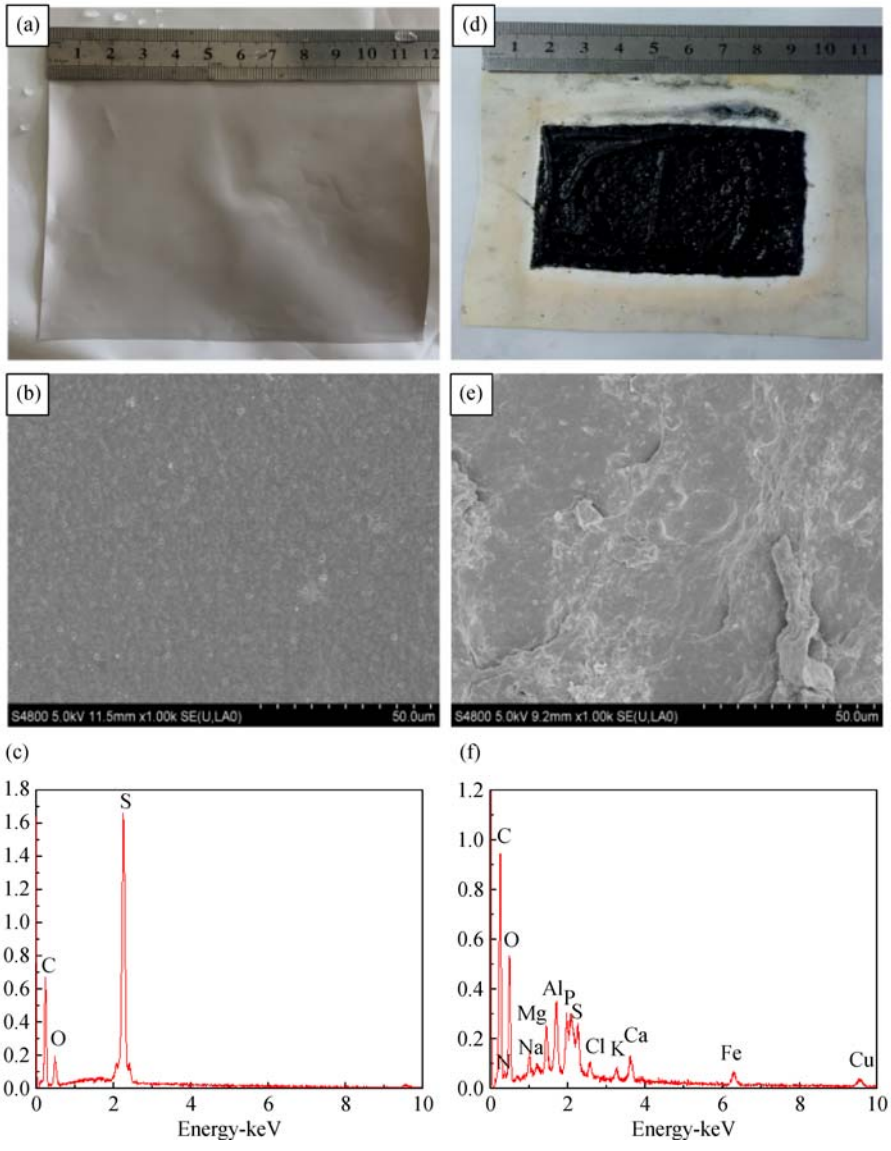

Fig. 5 Photoes, SEM images and EDX results of virgin (a, b, c) and fouled (d, e, f) FO membranes in the OsMFC

showed a great variety of elements in the fouling layer including C, O, N, Na, Mg, Al, P, S, Cl, K, Ca, Fe and Cu. There is one noteworthy fact that all the above elements existed on the fouled FO membrane could be found in the feed wastewater. Thus, influent wastewater was regarded as the main source of membrane foulants. Compared with the virgin one, the existence of N and metal cations such as Ca and Mg demonstrated the combined inorganic fouling and biofouling on the FO membrane surface (Wang et al., 2008, 2014a; Lin et al., 2012). To distinguish the different contributions of inorganic fouling and biofouling, the foulants on the FO membrane were collected and further analyzed. The MLVSS/MLSS ratio of the foulants was 0.76 (see Table S3), suggesting the biofouling including microorganisms, proteins and polysaccharides played a more significant role in the FO membrane fouling during the operation of OsMFC.

To further understand the biofouling of FO membrane in the OsMFC, the variations of α-D-glucopyranose and β-D-glucopyranose polysaccharides, proteins and microorganisms on the FO membrane surface were investigated by the CLSM combined with the multiple fluorescence probes. As shown in Fig. 6, the thickness of the fouling layer was about 90 μm. Although the fouling layer of FO membrane was thick, the fouling layer was loose. It could also be found from Fig. 6 that the proteins formed a continuous layer while the α-D-polysaccharide loosely distributed and appeared only in some spots on the FO membrane surface. Furthermore, the biovolume of polysaccharides, proteins and microorganisms was calculated by PHLIP. As shown in Table S4, the biovolume of proteins, β-D-glucopyranose polysaccharides and microorganisms was much larger than that of α-D-polysaccharide polysaccharides. These facts indicated that proteins, β-D-glucopyranose polysacchar-

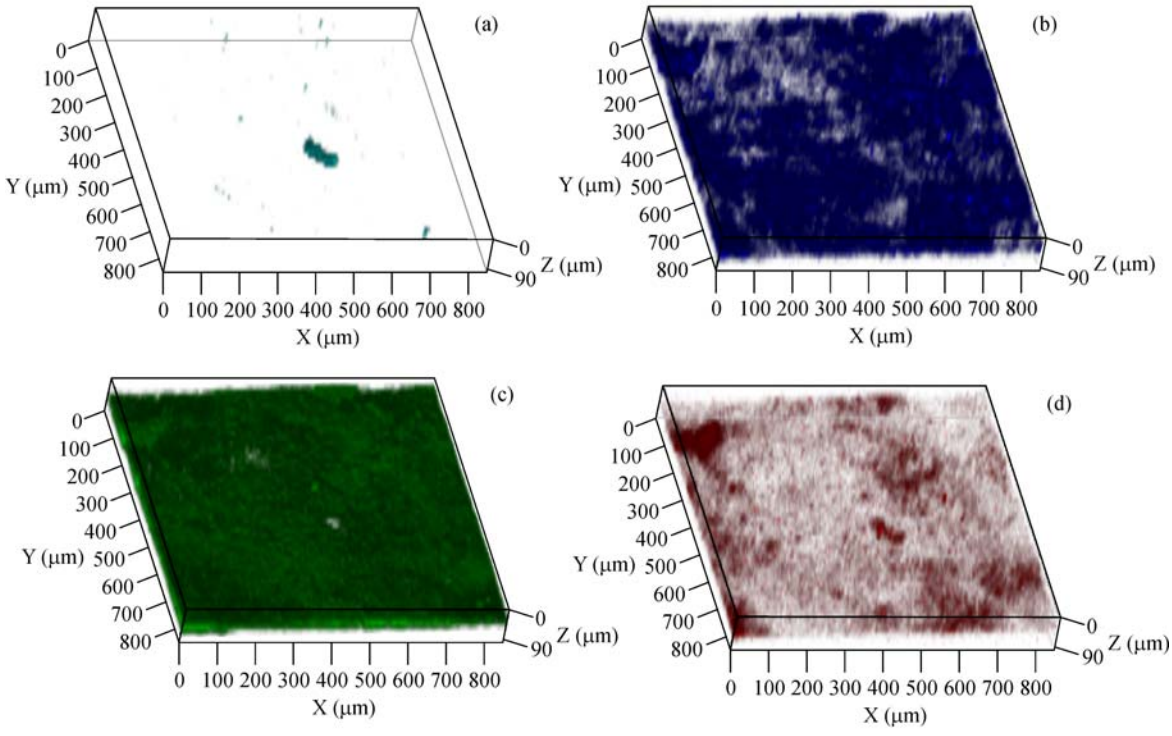

Fig. 6 CLSM images of α-D-glucopyranose polysaccharides (a), ß-D-glucopyranose polysaccharides (b), proteins (c) and total cells (d) in the FO fouling layer

ides and microorganisms were the major components of the biofoulants, implying that they played a more significant role in the formation and development of biofouling layer.

3.4 Development of biofouling layer

To further analyze the development of biofouling layer on the FO membrane surface, the CLSM images of biofoulants at different thicknesses of the fouling layer were analyzed. From Fig. 7, it can be concluded that the bacteria and the β-D-glucopyranose polysaccharides are the pioneers in the initial biofouling, and then the polysaccharides and proteins dramatic increased with the growth of the bacteria, finally, their concentrations decreased. Based on the above results and analyses, the development of fouling layer on the FO membrane surface in the OsMFC could be divided into three stages. As shown in Fig. 8, stage 1 was the deposition and attachment of microorganisms and their secretion of EPSs. The β-D-glucopyranose polysaccharides were easier to deposit on the FO membrane surface compared to the α-D-glucopyranose polysaccharides. During stage 2, the microorganisms subsequent growth into a biofilm caused the initial formation of biofouling layer on the FO membrane surface, in the meanwhile, a lot of proteins and polysaccharides significantly increased. Abundant of polysaccharide and proteins deposited on the membrane resulting in a quick decrease of water flux. However, when the operating time of the OsMFC was further lengthened (stage 3), some of microorganisms were dead due to lack of nutrient source and polysaccharide and proteins in the biofouling layer were decomposed as nutrient source. During stage 3, slight variation of FO membrane flux was observed, in which period the biofouling layer developed slowly. In all stages of the biofouling layer development, microorganisms played a significant role in the formation and development of the biofouling layer. Thus, it is necessary to pay more attentions on controlling the deposition and development of microorganisms on the FO membrane surface in order to enhance the FO membrane flux in the OsMFC.

4 Conclusions

The results of this study revealed that the membrane fouling on the FO membrane surface in the OsMFC played an important role in flux decline of FO membrane. Compared with the inorganic fouling, biofouling contributed more to the FO membrane fouling in the OsMFC. The biofoulants on the FO membrane surface included the polysaccharides, proteins and microorganisms. In the formation and development of the biofouling layer, the microorganisms and their secretion of EPSs first deposited on the FO membrane surface, and then the microorganisms subsequent growth into a biofilm caused the initial

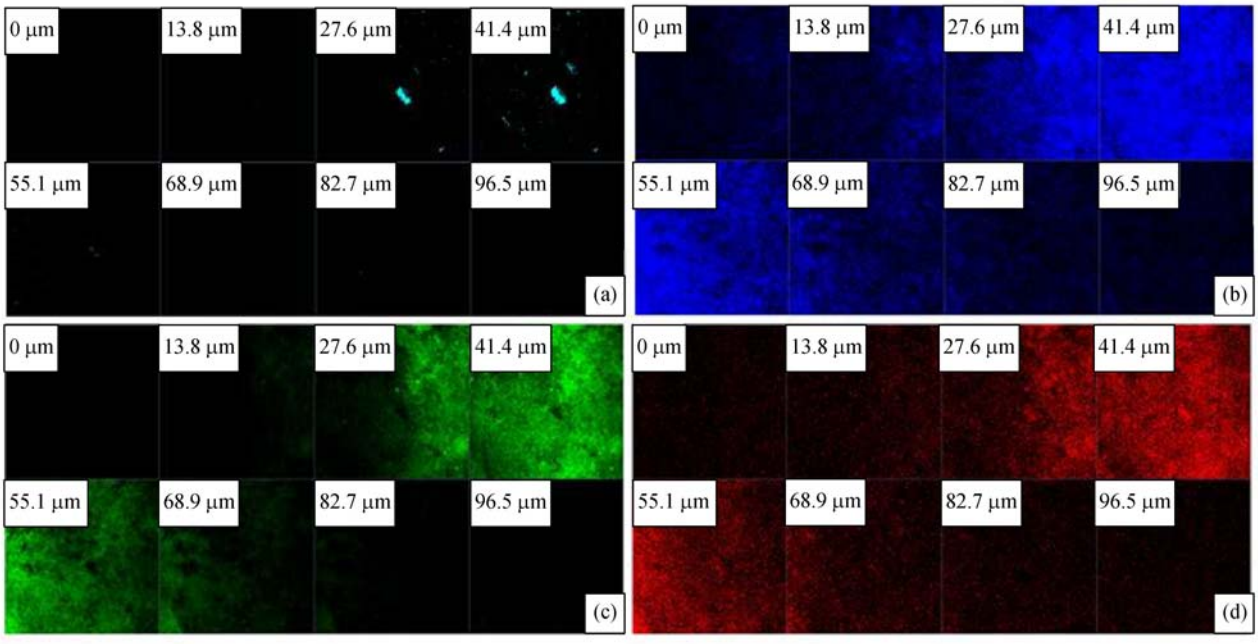

Fig. 7 CLSM images of α-D-glucopyranose polysaccharides (a), ß-D-glucopyranose polysaccharides (b), proteins (c) and total cells (d) at different thicknesses of fouling layer on the FO membrane surface

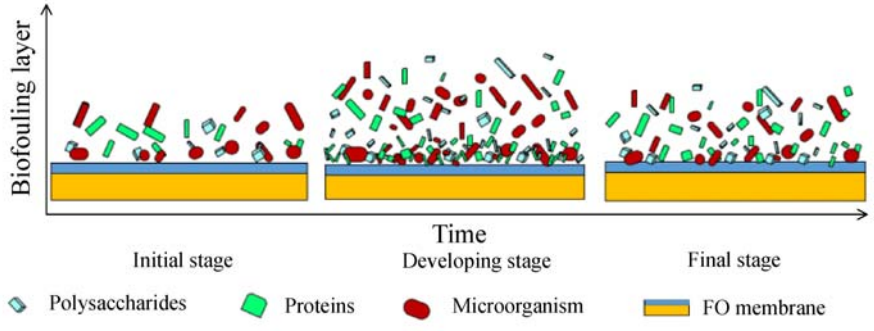

Fig. 8 Changes in the spatial and temporal distributions of bio-polymers and microorganisms in the cake layer in the OsMFC system

formation of biofouling layer on the FO membrane surface, in the meanwhile, a lot of proteins and polysaccharides significantly increased. Finally, some of microorganisms were dead due to lack of nutrient source and polysaccharide and proteins in the biofouling layer were decomposed as nutrient source. In all stages of the biofouling layer development, microorganisms played a significant role in the formation and development of the biofouling layer.

Acknowledgements This work was supported by the National Natural Science Foundation of China (Grant No. 51578265); the Fundamental Research Funds for the Central Universities (Grant No. JUSRP 51728A); the National Key Research and Development Program of China (Grant No. 2016YFC0400707); and Jiangsu Cooperative Innovation Center of Technology and Material of Water Treatment.

Electronic Supplementary Material Supplementary material is available in the online version of this article at https://doi.org/10.1007/s11783-018-1049-4 and is accessible for authorized users.

References

APHA (2012).Standard Methods for the Examination of Water and Wastewater. Washington, DC: American Public Health Association

Cath T Y, Childress A E, Elimelech M (2006). Forward osmosis: Principles, applications, and recent developments. J Membr Sci, 281 (1–2): 70–87

Chen L, Gu Y, Cao C, Zhang J, Ng J W, Tang C (2014). Performance of a submerged anaerobic membrane bioreactor with forward osmosis membrane for low-strength wastewater treatment. Water Res, 50: 114–123

Ge Z, He Z (2012). Effects of draw solutions and membrane conditions

on electricity generation and water flux in osmotic microbial fuel cells. Bioresour Technol, 109(2): 70–76

Ge Z, Ping Q Y, Xiao L, He Z (2013). Reducing effluent discharge and recovering bioenergy in an osmotic microbial fuel cell treating domestic wastewater. Desalination, 312: 52–59

He Z (2012). One more function for microbial fuel cells in treating wastewater: producing high-quality water. Chemik, 66: 7–10

Lefebvre O, Tan Z, Kharkwal S, Ng H Y (2012). Effect of increasing anodic NaCl concentration on microbial fuel cell performance. Bioresour Technol, 112(3): 336–340

Li W W, Yu H Q, He Z (2014). Towards sustainable wastewater treatment by using microbial fuel cells-centered technologies. Energy Environ Sci, 7(3): 911–924

Lin H, Gao W, Meng F, Liao B Q, Leung K T, Zhao L, Chen J, Hong H (2012). Membrane bioreactors for industrial wastewater treatment: A critical review. Crit Rev Environ Sci Technol, 42(7): 677–740

Liu J, Wang X, Wang Z, Lu Y, Li X, Ren Y (2017). Integrating microbial fuel cells with anaerobic acidification and forward osmosis membrane for enhancing bio-electricity and water recovery from low-strength wastewater. Water Res, 110: 74–82

Logan B E, Hamelers B, Rozendal R, Schröder U, Keller J, Freguia S, Aelterman P, Verstraete W, Rabaey K (2006). Microbial fuel cells: Methodology and technology. Environ Sci Technol, 40(17): 5181–5192

Mahan Y, Das D (2009). Effect of ionic strength, cation exchanger and inoculum age on the performance of microbial fuel cell. Int J Hydrogen Energy, 34(17): 7542–7546

Mccutcheon J R, Elimelech M (2006). Influence of concentrative and dilutive internal concentration polarization on flux behavior in forward osmosis. J Membr Sci, 284(1): 237–247

Mi B, Elimelech M (2008). Chemical and physical aspects of organic fouling of forward osmosis membranes. J Membr Sci, 320(1): 292–302

Pant D, Van Bogaert G, Diels L, Vanbroekhoven K (2010). A review of the substrates used in microbial fuel cells (MFCs) for sustainable energy production. Bioresour Technol, 101(6): 1533–1543

Qin M, Ping Q, Lu Y, Abu-Reesh I M, He Z (2015). Understanding electricity generation in osmotic microbial fuel cells through integrated experimental investigation and mathematical modeling. Bioresour Technol, 195: 194–201

Qin M H, Hynes E A, Abu-Reesh I M, He Z (2017). Ammonium removal from synthetic wastewater promoted by current generation and water flux in an osmotic microbial fuel cell. J Clean Prod, 149: 856–862

Tang C Y, She Q, Loong W C L, Wang R, Fane A G (2010). Coupled effects of internal concentration polarization and fouling on flux behavior of forward osmosis membranes during humic acid filtration. J Membr Sci, 354(1): 123–133

Wang X, Chen Y, Yuan B, Li X, Ren Y (2014b). Impacts of sludge retention time on sludge characteristics and membrane fouling in a submerged osmotic membrane bioreactor. Bioresour Technol, 161 (3): 340–347

Wang X, Hu T, Wang Z, Li X, Ren Y (2017a). Permeability recovery of fouled forward osmosis membranes by chemical cleaning during a long-term operation of anaerobic osmotic membrane bioreactors treating low-strength wastewater. Water Res, 123: 505–512

Wang X, Yuan B, Chen Y, Li X, Ren Y (2014a). Integration of microfiltration into osmotic membrane bioreactors to prevent salinity build-up. Bioresour Technol, 167(2): 116–123

Wang X, Zhao Y, Yuan B, Wang Z, Li X, Ren Y (2016b). Comparison of biofouling mechanisms between cellulose triacetate (CTA) and thin-film composite (TFC) polyamide forward osmosis membranes in osmotic membrane bioreactors. Bioresour Technol, 202: 50–58

Wang X H, Chang V W C, Tang C Y (2016a). Osmotic membrane bioreactor (OMBR) technology for wastewater treatment and reclamation: Advances, challenges, and prospects for the future. J Membr Sci, 504: 113–132

Wang X H, Wang C, Tang C Y, Li X F, Ren Y P (2017b). Development of a novel anaerobic membrane bioreactor simultaneously integrating microfiltration and forward membranes for low-strength wastewater treatment. J Membr Sci, 527: 1–7

Wang X H, Zhang J F, Chang V W C, She Q H, Tang C Y (2018). Removal of cytostatic drugs from wastewater by an anaerobic osmotic membrane bioreactor. Chem Eng J, 339: 153–161

Wang X H, Zhao Y X, Li X F, Ren Y P (2017c). Performance evaluation of a microfiltration-osmotic membrane bioreactor (MF-OMBR) during removing silver nanoparticles from simulated wastewater. Chem Eng J, 313: 171–178

Wang Z W, Wu Z C, Ying X, Tian L (2008). Membrane fouling in a submerged membrane bioreactor (MBR) under sub-critical flux operation: Membrane foulant and gel layer characterization. J Membr Sci, 325(1): 238–244

Werner C M, Logan B E, Saikaly P E, Amy G L (2013). Wastewater treatment, energy recovery and desalination using a forward osmosis membrane in an air-cathode microbial osmotic fuel cell. J Membr Sci, 428(428): 116–122

Xie M, Bar-Zeev E, Hashmi S M, Nghiem L D, Elimelech M (2015). Role of Reverse Divalent Cation Diffusion in Forward Osmosis Biofouling. Environ Sci Technol, 49(22): 13222–13229

Yang E, Chae K J, Alayande A B, Kim K Y, Kim I S (2016). Concurrent performance improvement and biofouling mitigation in osmotic microbial fuel cells using a silver nanoparticle-polydopamine coated forward osmosis membrane. J Membr Sci, 513: 217–225

Yuan B, Wang X, Tang C, Li X, Yu G (2015). In situ observation of the growth of biofouling layer in osmotic membrane bioreactors by multiple fluorescence labeling and confocal laser scanning microscopy. Water Res, 75: 188–200

Zhang F, Brastad K S, He Z (2011). Integrating forward osmosis into microbial fuel cells for wastewater treatment, water extraction and bioelectricity generation. Environ Sci Technol, 45(15): 6690–6696

Zhang F, Jacobson K S, Torres P, He Z (2010). Effects of anolyte recirculation rates and catholytes on electricity generation in a liter-scale upflow microbial fuel cell. Energy Environ Sci, 3(9): 1347–1352

Zhang J S, Loong W C L, Chou S, Tang C Y, Wang R, Fane A G (2012). Membrane biofouling and scaling in forward osmosis membrane bioreactor. J Membr Sci, 403: 8–14

Zhu W J, Wang X H, She Q H, Li X F, Ren Y P (2018). Osmotic membrane bioreactors assisted with microfiltration membrane for

salinity control (MF-OMBR) operating at high sludge concentrations: Performance and implications. Chem Eng J, 337: 576–583

Zhu X Z, Zhang F, Li W W, Li J, Li L L, Yu H Q, Huang M S, Huang T Y (2016). Insights into enhanced current generation of an osmotic microbial fuel cell under membrane fouling condition. J Membr Sci, 504: 40–46

Zhu X Z, Zhang F, Li W W, Liu H Q, Wang Y K, Huang M S (2015). Forward osmosis membrane favors an improved proton flux and electricity generation in microbial fuel cells. Desalination, 372: 26–31